

Editorial Article

Hartree-Fock methods analysis protonated rhodochrosite crystal and potential in the elimination of cancer cells through synchrotron radiation using Small-Angle X-Ray Scattering (SAXS), Ultra-Small Angle X-Ray Scattering (USAXS), Fluctuation X-Ray Scattering (FXS), Wide-Angle X-Ray Scattering (WAXS), Grazing-Incidence Small-Angle X-Ray Scattering (GISAXS), Grazing-Incidence Wide-Angle X-Ray Scattering (GIWAXS) and Small-Angle Neutron Scattering (SANS)

Corresponding author: Prof. Dr. Alireza Heidari*
Ricardo Gobato¹, Marcia Regina Risso Gobato¹, Abhijit Mitra²

**Faculty of Chemistry, California South University, 14731 Comet St. Irvine, CA 92604, USA*

¹Green Land Landscaping and Gardening, Seedling Growth Laboratory, 86130-000, Parana, Brazil

²Department of Marine Science, University of Calcutta, 35 B.C. Road Kolkata, 700019, India

Received on: 14-04-2020; Revised and Accepted on: 20-04-2020

ABSTRACT

The rhodochrosite (MnCO₃) shows complete solid solution with siderite (FeCO₃), and it may contain substantial amounts of Zn, Mg, Co, and Ca. The electric charge that accumulates in certain solid materials, such as crystals, certain ceramics, and biological matter such as bone, DNA and various proteins in response to applied mechanical stress, phenomenon called piezoelectricity. There is no precedent in the literature on the treatment of tumor tissues by eliminating these affected tissues, using rhodochrosite crystals in tissue absorption and eliminating cancerous tissues by synchrotron radiation. An in-depth study is necessary to verify the absorption by the tumoral and non-tumoral tissues of rhodochrosite, before and after irradiating of synchrotron radiation using Small-Angle X-Ray Scattering (SAXS), Ultra-Small Angle X-Ray Scattering (USAXS), Fluctuation X-Ray Scattering (FXS), Wide-Angle X-Ray Scattering (WAXS), Grazing-Incidence Small-Angle X-Ray Scattering (GISAXS), Grazing-Incidence Wide-Angle X-Ray Scattering (GIWAXS), Small-Angle Neutron Scattering (SANS), Grazing-Incidence Small-Angle Neutron Scattering (GISANS), X-Ray Diffraction (XRD), Powder X-Ray Diffraction (PXRD), Wide-Angle X-Ray Diffraction (WAXD), Grazing-Incidence X-Ray Diffraction (GIXD) and Energy-Dispersive X-Ray Diffraction (EDXRD). Later studies could check the advantages and disadvantages of rhodochrosite in the treatment of cancer through synchrotron radiation, such as one oscillator crystal. The studies that are found are the research papers of this team. Through an unrestricted Hartree-Fock (UHF) computational simulation, Compact effective potentials (CEP), the infrared spectrum of the protonated rhodochrosite crystal, CH₁₉Mn₆O₈, and the load distribution by the unit molecule by two widely used methods, Atomic Polar Tensor (APT) and Mulliken, were studied. The rhodochrosite crystal unit cell of structure CMn₆O₈, where the load distribution by the molecule was verified in the UHF CEP-4G (Effective core potential (ECP) minimal basis), UHF CEP-31G (ECP split valance) and UHF CEP-121G (ECP triple-split basis). The largest load variation in the APT and Mulliken methods were obtained in the CEP-121G basis set, with $\delta = 2.922$ e $\delta = 2.650$ u. a., respectively, being $\delta_{APT} > \delta_{Mulliken}$. The maximum absorbance peaks in the CEP-4G, CEP-31G and CEP-121G basis set are present at the frequencies 2172.23 cm⁻¹, with a normalized intensity of 0.65; 2231.4 cm⁻¹ and 0.454; and 2177.24 cm⁻¹ and 1.0, respectively. Studying the sites of rhodochrosite action may lead to a better understanding of its absorption by healthy and/or tumor tissues, thus leading to a better application of synchrotron radiation to the tumors to eliminate them.

KEYWORDS: Rhodochrosite, Quartz Crystal, Hartree-Fock Methods, APT, Mulliken, Effective core potential, Synchrotron Radiation, Cancer, Tumoral Tissues.

INTRODUCTION:

1. Introduction

The rhodochrosite (MnCO₃) shows complete solid solution with siderite (FeCO₃), and it may contain substantial amounts of Zn, Mg, Co, and Ca. The electric charge that accumulates in certain solid materials, such as crystals, certain ceramics, and biological matter such as bone, DNA and various proteins in response to applied mechanical stress, phenomenon called piezoelectricity. [1-12]

Through an unrestricted Hartree-Fock (UHF) computational simulation, Compact effective potentials (CEP), the infrared spectrum of the protonated rhodochrosite crystal, CH₁₉Mn₆O₈,

and the load distribution by the unit molecule by two widely used methods, Atomic Polar Tensor (APT) and Mulliken, were studied. The rhodochrosite crystal unit cell of structure CMn₆O₈, where the load distribution by the molecule was verified in the UHF CEP-4G (Effective core potential (ECP) minimal basis), UHF CEP-31G (ECP split valance) and UHF CEP-121G (ECP triple-split basis).

***Corresponding Author:**

Prof. Dr. Alireza Heidari,
Full Distinguished Professor and Academic Tenure of
Chemistry & Director of the BioSpectroscopy Core Research
Laboratory at Faculty of Chemistry,

California South University (CSU), Irvine, California, USA & President of the American International Standards Institute (AISI) Irvine, California, USA

E-mail: scholar.researcher.scientist@gmail.com

DOI: <https://doi.org/10.5281/zenodo.3757944>



Figure 1. Natural Pink w/Yellow Rhodochrosite Rough Specimen Gemstone Crystal Mineral Rock. Rhodochrosite from Santa Rita mine, Morococha District, Yauli Province, Junin Department, Peru. Weight: 650ct, dimensions: 59mm x 52mm x 36mm / 2 5/16 x 2 1/16 x 1 7/16 Inches; 130g / 4.6 oz. [13]

The Figure (1) is one photography the Rhodochrosite from Santa Rita mine, Morococha District, Yauli Province, Junin Department, Peru. Weight: 650ct. [13]



Figure 2. Rhodochrosite with Fluorite, Quartz and Pyrite Sweet Home Mine, main stope, Mount Bross, Alma District, Park County, Colorado USA (1993) Specimen size: 8.1 × 7 × 3.6 cm = 3.2" × 2.8" × 1.4" Main crystal size: 1.2 × 1.2 cm = 0.5" × 0.5" [14]

The Figure (2) is one photography the Rhodochrosite with Fluorite, Quartz and Pyrite stone, some cut and used with semi-precious jewelry. Sweet Home Mine, main stope, Mount Bross, Alma District, Park County, Colorado USA (1993) Specimen size: 8.1 × 7 × 3.6 cm = 3.2" × 2.8" × 1.4" Main crystal size: 1.2 × 1.2 cm = 0.5" × 0.5" [14]

2. Methods

2.1 Hartree-Fock Methods

The molecular Hartree-Fock [15-21] wave function is written as an antisymmetrized product (Slater determinant) of spin-orbitals, each spin-orbital being a product of a spatial orbital ϕ_i and a spin function (either α or β).

The expression for the Hartree-Fock molecular electronic energy E_{HF} is given by the variation theorem as $E_{HF} = \langle D | \hat{H}_{el} + V_{NN} | D \rangle$ where D is the Slater-determinant Hartree-Fock wave function and \hat{H}_{el} and V_{NN} are given by

$$\hat{H}_{el} = -\frac{\hbar^2}{2m_e} \sum_i \nabla_i^2 - \sum_\alpha \sum_i \frac{Z_\alpha e'^2}{r_{i\alpha}} + \sum_j \sum_{i>j} \frac{e'^2}{r_{ij}}$$

$$V_{NN} = \sum_\alpha \sum_{\beta>\alpha} \frac{Z_\alpha Z_\beta e'^2}{r_{\alpha\beta}}$$

Since V_{NN} does not involve electronic coordinates and D is normalized, we have $\langle D | V_{NN} | D \rangle = V_{NN} \langle D | D \rangle = V_{NN}$. The operator \hat{H}_{el} is the sum of one-electron operators \hat{f}_i and two-electron operators \hat{g}_{ij} ; we have $\hat{H}_{el} = \sum_i \hat{f}_i + \sum_j \sum_{i>j} \hat{g}_{ij}$, where $\hat{f}_i = -\frac{1}{2} \nabla_i^2 \sum_\alpha \sum_\alpha / r_{i\alpha}$ and $\hat{g}_{ij} = 1/r_{ij}$. The Hamiltonian \hat{H}_{el} is the same as the Hamiltonian \hat{H} for an atom except that $\sum_\alpha \sum_\alpha / r_{i\alpha}$ replaces Z/r_i in \hat{f}_i .

Therefore, the Hartree-Fock energy of a diatomic or polyatomic molecule with only closed shells is

$$E_{HF} = 2 \sum_{i=1}^{n/2} H_i^{core} + \sum_{j=1}^{n/2} \sum_{i=1}^{n/2} (2J_{ij} - K_{ij}) + V_{NN}$$

$$H_i^{core} \equiv \langle \phi_i(1) | \hat{H}^{core}(1) | \phi_i(1) \rangle \\ \equiv \langle \phi_i(1) | -\frac{1}{2} \nabla_i^2 \sum_\alpha Z_\alpha / r_{1\alpha} | \phi_i(1) \rangle$$

$$J_{ij} \equiv \langle \phi_i(1) \phi_j(2) | 1/r_{12} | \phi_i(1) \phi_j(2) \rangle$$

and

$$K_{ij} \equiv \langle \phi_i(1) \phi_j(2) | 1/r_{12} | \phi_j(1) \phi_i(2) \rangle$$

where the one-electron-operator symbol was changed from \hat{f}_i to $\hat{H}^{core}(1)$. [5]

3. Results and Discussion

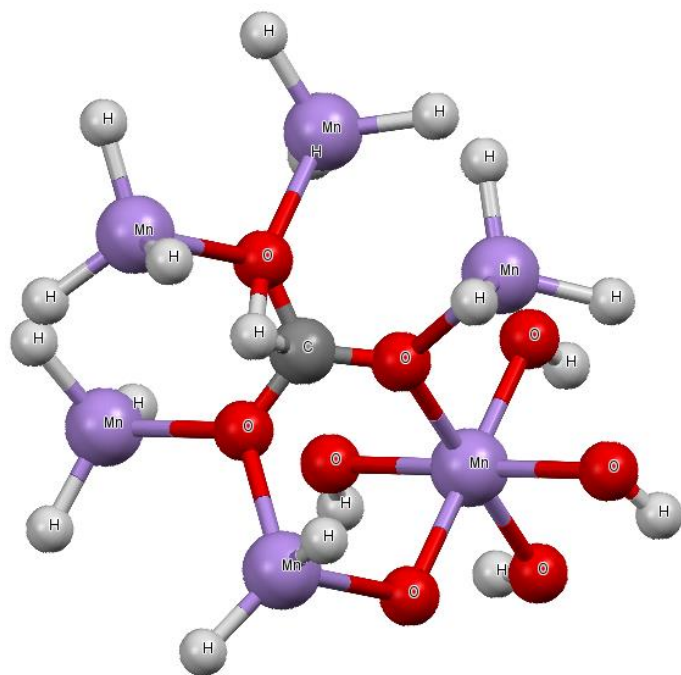


Figure 3. Cell structure of a protonated rhodochrosite crystal. Represented in red the oxygen; Purple in color Manganese; in gray color Hydrogen; in dark grey color the Carbon. Stoichiometry: CMn_6O_8 . Stoichiometry protonated: $\text{CH}_{19}\text{Mn}_6\text{O}_8$.

The Figure (3) show on cell structure of a protonated rhodochrosite crystal of structure Stoichiometric is $\text{CH}_{19}\text{Mn}_6\text{O}_8$, obtained after molecular dynamics via unrestricted Hartree-Fock method, in basis set CEP-4G, CEP-31G and CEP-121G. [32, 97]

The rhodochrosite crystal unit cell of structure CMn_6O_8 , where the load distribution by the molecule was verified in the unrestricted Hartree-Fock method, UHF CEP-4G (Effective core potential (ECP) minimal basis), UHF CEP-31G (ECP split valance) and UHF CEP-121G (ECP triple-split basis), through the analysis of APT and Mulliken loads [98-107].

The rhodochrosite unit cell was protonated, then presented the structure $\text{CH}_{19}\text{Mn}_6\text{O}_8$ for the study with *ab initio* methods with +4 multiplicity. The displacement of charges by the molecule was analyzed to verify the site of molecular action.

The load distribution by the protonated crystal is evaluated in Table (1), and its vibrational frequencies in Table (2).

Table 1. Load shifting on given basis sets of the Mulliken and APT method.

| Basis Sets | Mulliken | | | APT | | |
|------------|----------|--------|----------|---------|--------|----------|
| | Charge* | | δ | Charge* | | δ |
| CEP-4G | -1.064 | +1.064 | 2.128 | -1.366 | +1.366 | 2.732 |
| CEP-31G | -1.034 | +1.034 | 2.068 | -1.362 | +1.362 | 2.724 |

| | | | | | | |
|----------|--------|--------|-------|--------|--------|-------|
| CEP-121G | -1.325 | +1.325 | 2.650 | -1.461 | +1.461 | 2.922 |
|----------|--------|--------|-------|--------|--------|-------|

* $\pm 1,602\ 176\ 634 \times 10^{-19}$ C (Coulomb).

The largest load variation in the APT and Mulliken methods were obtained in the CEP-121G base set, with $\delta = 2.922$ e $\delta = 2.650$, respectively, being $\delta_{\text{APT}} > \delta_{\text{Mulliken}}$, in all sets of calculated bases, Table (1).

Table 2. Peaks maximum absorption intensity by the frequency given. Absorbance frequency as a function of vibrational frequencies of protonated rhodochrosite crystal for UHF-CEP-4G basis set, UHF-CEP-31G and UHF-CEP-121G.

| | ν (cm^{-1}) | I (%) | ν (cm^{-1}) | I (%) | ν (cm^{-1}) | I (%) | ν (cm^{-1}) | I (%) |
|----------|----------------------------|-------------|----------------------------|-------------|----------------------------|-------------|----------------------------|-------------|
| CEP-4G | 217 2.23 | 64.9 904 | 204 3.25 | 51.7 671 | 219 3.1 | 41.6 608 | 224 2.97 | 36.4 643 |
| CEP-31G | 223 1.4 | 45.3 589 | 189 1.26 | 41.6 207 | 202 7.77 | 40.3 978 | 192 6.32 | 38.0 064 |
| CEP-121G | 217 7.24 | 100 | 226 1.98 | 87.0 553 | 194 7.03 | 83.1 151 | 177 8.57 | 51.6 624 |

ν = Frequency (cm^{-1}); I = Normalized Intensity (%).

The Table (2) show the maximum absorbance peaks in the CEP-4G, CEP-31G and CEP-121G set basis are present at the frequencies $2172.23\ \text{cm}^{-1}$, with a normalized intensity of 65%; $2231.4\ \text{cm}^{-1}$ and 45.4%; and $2177.24\ \text{cm}^{-1}$ and 100%, respectively.

4. Analysis

The Mulliken load method in the UHF-CEP-4G base set; UHF-CEP-31G and UHF-CEP-121G are sufficient to show that the sites of action of the rhodochrosite crystal structure are found in three Oxygen-linked Manganese atoms, which are attached to the central Carbon atom, as well as these. Oxygen atoms and the central Carbon.

These Manganese atoms show a slight negative to neutral load shift in the CEP-4G set basis, neutral to positive in the CEP-31G and CEP-121G set basis at the Mulliken charges.

The charge displacement is strong in the oxygen atoms, especially those near the central carbon, with negative load in all set basis studied, both in the APT and Mulliken charges.

The central carbon atom on all set basis is positively charged in both APT and Mulliken load, except Mulliken in CEP-31G, which is neutral.

As might be expected from the charges by APT, the strong positive load manganese atoms, the strong negative load oxygen, the

positively charged carbon atom. The manganese atom farthest from the carbon atom has a slight positive to neutral load shift.

The Mulliken load method presents a better result when compared to the APT, in the studied set basis, for protonated rhodochrosite crystal, with a smaller load variation $\delta = 2,650$ u.a for CEP-121G.

The absorption peaks are in a Gaussian between the frequencies 1620 cm^{-1} and 2520 cm^{-1} , Figure 3D.

The largest load variation in the APT and Mulliken methods were obtained in the CEP-121G base set, with $\delta = 2.922$ e $\delta = 2.650$, respectively, being $\delta_{\text{APT}} > \delta_{\text{Mulliken}}$, in all sets of calculated basis, Table (1).

The Figure (1) is one photography the Rhodochrosite stone from China.

The Figure (2) is one photography the Rhodochrosite with Fluorite, Quartz and Pyrite stone, some cut and used with semi-precious jewelry. Sweet Home Mine, main stope, Mount Bross, Alma District, Park County, Colorado USA (1993) Specimen size: $8.1 \times 7 \times 3.6\text{ cm} = 3.2'' \times 2.8'' \times 1.4''$ Main crystal size: $1.2 \times 1.2\text{ cm} = 0.5'' \times 0.5''$ [14]

The Figure (3) represented a Cell structure of a protonated rhodochrosite crystal. Represented in red the oxygen; silver in color Manganese; in gray color Hydrogen; in light see green color the Carbon. Stoichiometry not protonated: CMn_6O_8 . Stoichiometry protonated: $\text{CH}_{19}\text{Mn}_6\text{O}_8$.

The rhodochrosite crystal unit cell of structure CMn_6O_8 , where the load distribution by the molecule was verified in the unrestricted Hartree-Fock method, UHF CEP-4G (Effective core potential (ECP) minimal basis), UHF CEP-31G (ECP split valance) and UHF CEP-121G (ECP triple-split basis), through the analysis of APT and Mulliken loads.

5. Conclusion

The absorption peaks are in a Gaussian between the frequencies 1620 cm^{-1} and 2520 cm^{-1} .

The Mulliken load method presents a better result when compared to the APT, in the studied set basis, for protonated rhodochrosite crystal, with a smaller load variation $\delta = 2,650$ u.a for CEP-121G.

The maximum absorbance peaks in the CEP-4G, CEP-31G and CEP-121G set basis are present at the frequencies 2172.23 cm^{-1} , with a normalized intensity of 0.65, 2231.4 cm^{-1} and 0.454 and 2177.24 cm^{-1} and 1.0 respectively.

Later studies could check the advantages and disadvantages of rhodochrosite in the treatment of cancer through synchrotron radiation, such as one oscillator crystal.

An in-depth study is necessary to verify the absorption by the tumoral and non-tumoral tissues of rhodochrosite, before and after irradiating of synchrotron radiation using Small-Angle X-Ray Scattering (SAXS), Ultra-Small Angle X-Ray Scattering (USAXS), Fluctuation X-Ray Scattering (FXS), Wide-Angle X-Ray Scattering (WAXS), Grazing-Incidence Small-Angle X-Ray Scattering (GISAXS), Grazing-Incidence Wide-Angle X-Ray Scattering (GIWAXS), Small-Angle Neutron Scattering (SANS), Grazing-Incidence Small-Angle Neutron Scattering (GISANS), X-

Ray Diffraction (XRD), Powder X-Ray Diffraction (PXRD), Wide-Angle X-Ray Diffraction (WAXD), Grazing-Incidence X-Ray Diffraction (GIXD) and Energy-Dispersive X-Ray Diffraction (EDXRD).

References

- [1] F. James Holler, Douglas A. Skoog and Stanley R. Crouch. Principles of Instrumental Analysis (6th ed.). Cengage Learning. 200, p. 9. ISBN 978-0-495-01201-6.
- [2] Fox Electronics. Quartz Crystal Theory of Operation and Design Notes. Oscillator Theory of Operation and Design Notes. 2008. Available in: April 16, 2019. URL: <https://web.archive.org/web/20110725032851/http://www.foxonline.com/techdata.htm>.
- [3] R. E. Newnham. Properties of materials. Anisotropy, Symmetry, Structure. Oxford University Press, New York, 2005.
- [4] C. D. Gribble and A. J. Hall. A Practical Introduction to Optical Mineralogy. 1985.
- [5] Creative Commons. (CC-BY 4.0). Wikipedia, The Free Encyclopedia, May 2019. URL: <https://creativecommons.org/licenses/by/4.0/>.
- [6] Ricardo Gobato, Marcia Regina Risso Gobato, Alireza Heidari. Rhodochrosite as Crystal Oscillator. Am J Biomed Sci & Res. 2019 - 3 (2). AJBSR. MS. ID. 000659. DOI: 10.34297/AJBSR.2019.03.000659.
- [7] Ricardo Gobato, Marcia Regina Risso Gobato, Alireza Heidari. Calculation by UFF method of frequencies and vibrational temperatures of the unit cell of the rhodochrosite crystal International Journal of Advanced Chemistry, 7 (2) (2019) 77-81. doi: 10.14419/ijac.v7i1.29176.
- [8] Ricardo Gobato, Marcia Regina Risso Gobato, Alireza Heidari. Rhodochrosite as Crystal Oscillator. June 17, 2019. URL: https://www.researchgate.net/publication/333817526_Rhodochrosite_as_Crystal_Oscillator?enrichId=rgreq-26dd55b5b6e53fd29f8cf00042058725-XXX&enrichSource=Y292ZXJQYWdlOzMzMzgxNzUyNjBUzo3NzA3NDE0MTkxMjY3ODRAMTU2MDc3MDQ4MjgwOA%3D%3D&l=1_x_2&_esc=publicationCoverPdf.
- [9] Ricardo Gobato, Marcia Regina Risso Gobato, Alireza Heidari. Rhodochrosite as Crystal Oscillator. Am J Biomed Sci & Res. 2019 - 3(2). DOI: 10.34297/AJBSR.2019.03.000659.
- [10] Ricardo Gobato, Marcia Regina Risso Gobato, Alireza Heidari. Rhodochrosite as Crystal Oscillator. viXra.org, Condensed Matter, viXra: 1908.0295. <http://vixra.org/abs/1908.0295>.
- [11] Ricardo Gobato, Marcia Regina Risso Gobato, Alireza Heidari, Abhijit Mitra. Rhodochrosite Optical Indicatrix. Peer Res Nest. 2019 - 1 (3). PNEST. 19.08.020.
- [12] Ricardo Gobato, Marcia Regina Risso Gobato, Alireza Heidari, Abhijit Mitra. Rhodochrosite Optical Indicatrix. viXra.org > Condensed Matter > viXra: 1908.0455. URL: <http://vixra.org/abs/1908.0455>. Available in: Aug 22, 2019.
- [13] Amazon.com, CC-BY-SA-3.0. 2010. URL: <https://www.amazon.com/Natural-Rhodochrosite-Specimen-Gemstone-Crystal/dp/B07V4FSWBC>. Available in: Aug 22, 2019.

- [14] Fabre Minerals. 2020. Available in: February 20, 2020. URL: <https://www.fabreminerals.com/LargePhoto.php?FILE=Rhodochrosite-EN87A18d2.jpg&LANG=EN>.
- [15] I. N. Levine. Quantum Chemistry. Pearson Education (Singapore) Pte. Ltd., Indian Branch, 482 F. I. E. Patparganj, Delhi 110 092, India, 5th ed. edition, 2003.
- [16] A. Szabo and N. S. Ostlund. Modern Quantum Chemistry. Dover Publications, New York, 1989.
- [17] M. S. Gordon et al. General atomic and molecular electronic structure system (GAMESS). J. Comput. Chem., 14: 1347–1363, 1993.
- [18] K. Ohno, K. Esfarjani and Y. Kawazoe. Computational Material Science. Springer-Verlag, Berlin, 1999.
- [19] K. Wolfram and M. C. Hothausen. Introduction to DFT for Chemists. John Wiley & Sons, Inc. New York, 2nd ed. edition, 2001.
- [20] P. Hohenberg and W. Kohn. Inhomogeneous electron gas. Phys. Rev., (136): B864–B871, 1964.
- [21] W. Kohn and L. J. Sham. Self-consistent equations including exchange and correlation effects. Phys. Rev., (140): A1133, 1965.
- [22] R. S. Mulliken, J. Chem. Phys. 1955 23, 1833-1840.
- [23] I. G. Csizmadia, Theory and Practice of MO Calculations on Organic Molecules, Elsevier, Amsterdam, 1976.
- [24] Ferreira, M. M. C. J. Phys. Chem. 1990, 94, 3220-3223.
- [25] Biarge, J. F.; Herranz, J.; Morcillo, J. An. R. Soc. Esp. Fis. Quim. Ser. A 1961, A57, 81.
- [26] Person, W. B.: Newton, J. H. J. Chem. Phys. 1974, 61. 1040.
- [27] King, W. T.; Mast, G. B. J. Phys. Chem. 1976, 80, 2521.
- [28] King, W. T. Vibrational Intensities in Infrared and Raman Spectra: Person, W. B., Zerbi, G. Eds.; Elsevier: Amsterdam, 1982; Chapter 6.
- [29] Person, W. B.; Zilles, B.; Rogers, J. D.; Maia, R. G. A. J. Mol. Struct. 1982, 80, 297.
- [30] Zilles. B. A. Ph. D. Dissertation, University of Florida, 1980.
- [31] Zilles, B. A.; Person, W. B. J. Chem. Phys. 1983, 79, 65.
- [32] Ricardo Gobato, Marcia Regina Risso Gobato, Alireza Heidari, Abhijit Mitra. "Hartree-fock Methods Analysis Protonated Rhodochrosite Crystal and Potential in the Elimination of Cancer Cells Through Synchrotron Radiation", Radiation Science and Technology. Vol. 5, No. 3, 2019, pp. 27-36. doi: 10.11648/j.rst.20190503.12.
- [33] Ricardo Gobato, Ibtihal Kadhim Kareem Dosh, Alireza Heidari, Abhijit Mitra, Marcia Regina Risso Gobato. "Perspectives on the Elimination of Cancer Cells Using Rhodochrosite Crystal Through Synchrotron Radiation, and Absorption of the Tumoral and Non-Tumoral Tissues", Arch Biomed Eng & Biotechnol. 3(2): 2019. ABEB.MS.ID.000558. DOI: 10.33552/ABEB.2019.03.000558.
- [34] M. S. Gordon and M. W. Schmidt. Advances in electronic structure theory: GAMESS a decade later. Theory and Applications of Computational Chemistry: the first forty years. Elsevier. C. E. Dykstra, G. Frenking, K. S. Kim and G. E. Scuseria (editors), pages 1167–1189, 2005. Amsterdam.
- [35] R. Gobato, A. Gobato, D. F. G. Fedrigo, "Inorganic arrangement crystal beryllium, lithium, selenium and silicon". In XIX Semana da Física. Simpósio Comemorativo dos 40 anos do Curso de Física da Universidade Estadual de Londrina, Brazil, 2014. Universidade Estadual de Londrina (UEL).
- [36] R. Gobato, "Benzocafna, um estudo computacional", Master's thesis, Universidade Estadual de Londrina (UEL), 2008.
- [37] R. Gobato, "Study of the molecular geometry of Caramboxin toxin found in star flower (Averrhoa carambola L.)". Parana J. Sci. Edu, 3 (1): 1–9, January 2017.
- [38] R. Gobato, A. Gobato, D. F. G. Fedrigo, "Molecular electrostatic potential of the main monoterpenoids compounds found in oil Lemon Tahiti - (Citrus Latifolia Var Tahiti)". Parana J. Sci. Edu., 1 (1): 1–10, November 2015.
- [39] R. Gobato, D. F. G. Fedrigo, A. Gobato, "Allocryptopine, Berberine, Chelerythrine, Copsitine, Dihydrosanguinarine, Protopine and Sanguinarine. Molecular geometry of the main alkaloids found in the seeds of Argemone Mexicana Linn". Parana J. Sci. Edu., 1 (2): 7–16, December 2015.
- [40] R. Gobato, A. Heidari, "Infrared Spectrum and Sites of Action of Sanguinarine by Molecular Mechanics and ab initio Methods", International Journal of Atmospheric and Oceanic Sciences. Vol. 2, No. 1, 2018, pp. 1-9. doi: 10.11648/j.ijaos.20180201.11.
- [41] R. Gobato, D. F. G. Fedrigo, A. Gobato, "Molecular geometry of alkaloids present in seeds of mexican prickly poppy". Cornell University Library. Quantitative Biology, Jul 15, 2015. arXiv: 1507.05042.
- [42] R. Gobato, A. Gobato, D. F. G. Fedrigo, "Study of the molecular electrostatic potential of D-Pinitol an active hypoglycemic principle found in Spring flower Three Marys (Bougainvillea species) in the Mm+ method". Parana J. Sci. Educ., 2 (4): 1–9, May 2016.
- [43] R. Gobato, D. F. G. Fedrigo, A. Gobato, "Avro: key component of Lockheed X-35", Parana J. Sci. Educ., 1 (2): 1–6, December 2015.
- [44] R. Gobato, D. F. G. Fedrigo, A. Gobato, "LOT-G3: Plasma Lamp, Ozonator and CW Transmitter", Ciencia e Natura, 38 (1), 2016.
- [45] R. Gobato, "Matter and energy in a non-relativistic approach amongst the mustard seed and the faith. A metaphysical conclusion". Parana J. Sci. Educ., 2 (3): 1–14, March 2016.
- [46] R. Gobato, A. Gobato, D. F. G. Fedrigo, "Harnessing the energy of ocean surface waves by Pelamis System", Parana J. Sci. Educ., 2 (2): 1–15, February 2016.
- [47] R. Gobato, A. Gobato, D. F. G. Fedrigo, "Mathematics for input space probes in the atmosphere of Gliese 581d", Parana J. Sci. Educ., 2 (5): 6–13, July 2016.
- [48] R. Gobato, A. Gobato, D. F. G. Fedrigo, "Study of tornadoes that have reached the state of Parana". Parana J. Sci. Educ., 2 (1): 1–27, 2016.
- [49] R. Gobato, M. Simões F. "Alternative Method of RGB Channel Spectroscopy Using a CCD Reader", Ciencia e Natura, 39 (2), 2017.
- [50] R. Gobato, A. Heidari, "Calculations Using Quantum Chemistry for Inorganic Molecule Simulation BeLi2SeSi", Science Journal of Analytical Chemistry, 5 (5): 76–85, September 2017.

- [51] M. R. R. Gobato, R. Gobato, A. Heidari, "Planting of Jaboticaba Trees for Landscape Repair of Degraded Area", *Landscape Architecture and Regional Planning*, 3 (1): 1–9, March 18, 2018.
- [52] R. Gobato, "The Liotropic Indicatrix", 2012, 114 p. Thesis (Doctorate in Pysics). Universidade Estadual de Londrina, Londrina, 2012.
- [53] R. Gobato, A. Heidari, "Calculations Using Quantum Chemistry for Inorganic Molecule Simulation BeLi2SeSi", *Science Journal of Analytical Chemistry*, Vol. 5, No. 6, Pages 76–85, 2017.
- [54] R. Gobato, "O universo dos cristais líquidos", *Cadernos PDE*, Secretaria de Estado da Educação do Paraná, Vol. 2, Pages 1–15, 2009. ISBN 978-85-8015-053-7.
www.diaadiaeducacao.pr.gov.br/2009_uel_fisica_md_ricardo_gobato.
- [55] R. Gobato, A. Heidari, "Molecular Mechanics and Quantum Chemical Study on Sites of Action of Sanguinarine Using Vibrational Spectroscopy Based on Molecular Mechanics and Quantum Chemical Calculations", *Malaysian Journal of Chemistry*, Vol. 20 (1), 1–23, 2018.
- [56] A. Heidari, R. Gobato. "A Novel Approach to Reduce Toxicities and to Improve Bioavailabilities of DNA/RNA of Human Cancer Cells-Containing Cocaine (Coke), Lysergide (Lysergic Acid Diethyl Amide or LSD), Δ^9 -Tetrahydrocannabinol (THC) [(–)-trans- Δ^9 -Tetrahydrocannabinol], Theobromine (Xantheose), Caffeine, Aspartame (APM) (NutraSweet) and Zidovudine (ZDV) [Azidothymidine (AZT)] as Anti-Cancer Nano Drugs by Coassembly of Dual Anti-Cancer Nano Drugs to Inhibit DNA/RNA of Human Cancer Cells Drug Resistance", *Parana Journal of Science and Education*, v. 4, n. 6, pp. 1–17, 2018.
- [57] A. Heidari, R. Gobato, "Ultraviolet Photoelectron Spectroscopy (UPS) and Ultraviolet-Visible (UV-Vis) Spectroscopy Comparative Study on Malignant and Benign Human Cancer Cells and Tissues with the Passage of Time under Synchrotron Radiation", *Parana Journal of Science and Education*, v. 4, n. 6, pp. 18–33, 2018.
- [58] R. Gobato, A. Heidari, "Using the Quantum Chemistry for Genesis of a Nano Biomembrane with a Combination of the Elements Be, Li, Se, Si, C and H", *J Nanomed Res.*, 7 (4): 241-252, 2018.
- [59] S. K. Agarwal, S. Roy, P. Pramanick, P. Mitra, R. Gobato, A. Mitra, "Marsilea quadrifolia: A floral species with unique medicinal properties", *Parana J. Sci. Educ.*, v. 4, n. 5, (15–20), July 1, 2018.
- [60] A. Mitra, S. Zaman, R. Gobato. "Indian Sundarban Mangroves: A potential Carbon Scrubbing System". *Parana J. Sci. Educ.*, v. 4, n. 4, (7–29), June 17, 2018.
- [61] O. Yarman, R. Gobato, T. Yarman, M. Arik. "A new Physical constant from the ratio of the reciprocal of the "Rydberg constant" to the Planck length". *Parana J. Sci. Educ.*, v. 4, n. 3, (42–51), April 27, 2018.
- [62] R. Gobato, M. Simões F., "Alternative Method of Spectroscopy of Alkali Metal RGB", *Modern Chemistry*. Vol. 5, No. 4, 2017, pp. 70–74. <https://doi.org/10.11648/j.mc.20170504.13>.
- [63] D. F. G. Fedrigo, R. Gobato, A. Gobato, "Avrocar: a real flying saucer", *Cornell University Library*. 24 Jul 2015. arXiv: 1507.06916v1 [physics.pop-ph].
- [64] M, Simões F., A. J. Palangana, R. Gobato, O. R. Santos, "Micellar shape anisotropy and optical indicatrix in reentrant isotropic–nematic phase transitions", *The Journal of Chemical Physics*, 137, 204905 (2012); <https://doi.org/10.1063/1.4767530>.
- [65] A. Heidari, R. Gobato, "Putrescine, Cadaverine, Spermine and Spermidine-Enhanced Precatalyst Preparation Stabilization and Initiation (EPPSI) Nano Molecules", *Parana Journal of Science and Education (PJSE)*–v. 4, n. 5, (1–14) July 1, 2018.
- [66] R. Gobato, A. Heidari, A. Mitra, "The Creation of C13H20BeLi2SeSi. The Proposal of a Bio-Inorganic Molecule, Using Ab Initio Methods for the Genesis of a Nano Membrane", *Arc Org Inorg Chem Sci* 3 (4). AOICS. MS. ID. 000167, 2018.
- [67] R. Gobato, A. Heidari, A. Mitra, "Using the Quantum Chemistry for Genesis of a Nano Biomembrane with a Combination of the Elements Be, Li, Se, Si, C and H", *ResearchGate*, See discussions, stats, and author profiles for this publication at: <https://www.researchgate.net/publication/326201181>, 2018.
- [68] A. Heidari, R. Gobato, "First-Time Simulation of Deoxyuridine Monophosphate (dUMP) (Deoxyuridylic Acid or Deoxyuridylate) and Vomitoxin (Deoxynivalenol (DON)) ((3 α ,7 α)-3,7,15-Trihydroxy-12,13-Epoxytrichothec-9-En-8-One)-Enhanced Precatalyst Preparation Stabilization and Initiation (EPPSI) Nano Molecules Incorporation into the Nano Polymeric Matrix (NPM) by Immersion of the Nano Polymeric Modified Electrode (NPME) as Molecular Enzymes and Drug Targets for Human Cancer Cells, Tissues and Tumors Treatment under Synchrotron and Synchrocyclotron Radiations", *Parana Journal of Science and Education*, Vol. 4, No. 6, pp. 46–67, 2018.
- [69] R. Gobato, M. R. R. Gobato, A. Heidari, A. Mitra, "Spectroscopy and Dipole Moment of the Molecule C13H20BeLi2SeSi via Quantum Chemistry Using Ab Initio, Hartree-Fock Method in the Base Set CC-pVTZ and 6–311G**(3df, 3pd)", *American Journal of Quantum Chemistry and Molecular Spectroscopy*, Vol. 2, No. 1, pp. 9–17, 2018.
- [70] R. Gobato, M. R. R. Gobato, A. Heidari, "Raman Spectroscopy Study of the Nano Molecule C13H20BeLi2SeSi Using ab initio and Hartree-Fock Methods in the Basis Set CC-pVTZ and 6–311G**(3df, 3pd)", *International Journal of Advanced Engineering and Science*, Volume 7, Number 1, Pages 14–35, 2019.
- [71] A. Heidari, R. Gobato, "Evaluating the Effect of Anti-Cancer Nano Drugs Dosage and Reduced Leukemia and Polycythemia Vera Levels on Trend of the Human Blood and Bone Marrow Cancers under Synchrotron Radiation", *Trends in Res*, Volume 2 (1): 1–8, 2019.
- [72] A. Heidari, R. Gobato, "Assessing the Variety of Synchrotron, Synchrocyclotron and LASER Radiations and Their Roles and Applications in Human Cancer Cells, Tissues and Tumors Diagnosis and Treatment", *Trends in Res*, Volume 2 (1): 1–8, 2019.
- [73] A. Heidari, R. Gobato, "Pros and Cons Controversy on Malignant Human Cancer Cells, Tissues and Tumors Transformation Process to Benign Human Cancer Cells, Tissues and Tumors", *Trends in Res*, Volume 2 (1): 1–8, 2019.
- [74] A. Heidari, R. Gobato, "Three-Dimensional (3D) Simulations of Human Cancer Cells, Tissues and Tumors for Using in Human Cancer Cells, Tissues and Tumors Diagnosis and Treatment as a Powerful Tool in Human Cancer Cells, Tissues and Tumors Research and Anti-Cancer Nano Drugs Sensitivity and Delivery

Area Discovery and Evaluation”, Trends in Res, Volume 2 (1): 1-8, 2019.

[75] A. Heidari, R. Gobato, “Investigation of Energy Production by Synchrotron, Synchrocyclotron and LASER Radiations in Human Cancer Cells, Tissues and Tumors and Evaluation of Their Effective on Human Cancer Cells, Tissues and Tumors Treatment Trend”, Trends in Res, Volume 2 (1): 1-8, 2019.

[76] A. Heidari, R. Gobato, “High-Resolution Mapping of DNA/RNA Hypermethylation and Hypomethylation Process in Human Cancer Cells, Tissues and Tumors under Synchrotron Radiation”, Trends in Res, Volume 2 (2): 1-9, 2019.

[77] R. Gobato, M. R. R. Gobato, A. Heidari, “Storm Vortex in the Center of Paraná State on June 6, 2017: A Case Study”, Sumerianz Journal of Scientific Research, Vol. 2, No. 2, Pages 24-31, 2019.

[78] R. Gobato, M. R. R. Gobato, A. Heidari, “Attenuated Total Reflection-Fourier Transform Infrared (ATR-FTIR) Spectroscopy Study of the Nano Molecule C₁₃H₂₀BeLi₂SeSi Using ab initio and Hartree-Fock Methods in the Basis Set RHF/CC-pVTZ and RHF/6-311G** (3df, 3pd): An Experimental Challenge to Chemists”, Chemistry Reports, Vol. 2, No. 1, Pages 1-26, 2019.

[79] R. Gobato, M. R. R. Gobato, A. Heidari, A. Mitra, “New Nano-Molecule Kurumi-C₁₃H₂₀BeLi₂SeSi/C₁₃H₁₉BeLi₂SeSi, and Raman Spectroscopy Using ab initio, Hartree-Fock Method in the Base Set CC-pVTZ and 6-311G** (3df, 3pd)”, J Anal Pharm Res. 8 (1): 1-6, 2019.

[80] R. Gobato, M. R. R. Gobato, A. Heidari, “Evidence of Tornado Storm Hit the Counties of Rio Branco do Ivaí and Rosario de Ivaí, Southern Brazil”, Sci Lett 7 (1), 9 Pages, 2019.

[81] Moharana Choudhury, Pardis Fazli, Prosenjit Pramanick, Ricardo Gobato, Sufia Zaman, Abhijit Mitra, “Sensitivity of the Indian Sundarban mangrove ecosystem to local level climate change”, Parana Journal of Science and Education. Vol. 5, No. 3, 2019, pp. 24-28.

[82] Arpita Saha, Ricardo Gobato, Sufia Zaman, Abhijit Mitra, “Biomass Study of Mangroves in Indian Sundarbans: A Case Study from Satjelia Island”, Parana Journal of Science and Education. Vol. 5, No. 2, 2019, pp. 1-5.

[83] Nabonita Pal, Arpan Mitra, Ricardo Gobato, Sufia Zaman, Abhijit Mitra, “Natural Oxygen Counters in Indian Sundarbans, the Mangrove Dominated World Heritage Site”, Parana Journal of Science and Education. Vol. 5, No. 2, 2019, pp. 6-13.

[84] Ricardo Gobato, Victoria Alexandrovna Kuzmicheva, Valery Borisovich Morozov, “Einstein's hypothesis is confirmed by the example of the Schwarzschild problem”, Parana Journal of Science and Education, Vol. 5, No. 1, 2019, pp. 1-6.

[85] Sufia Zaman, Ricardo Gobato, Prosenjit Pramanick, Pavel Biswas, Uddalok Chatterjee, Shampa Mitra, Abhijit Mitra, “Water quality of the River Ganga in and around the city of Kolkata during and after Goddess Durga immersion”, Parana Journal of Science and Education, Vol. 4, No. 9, 2018, pp. 1-7.

[86] Ozan Yarman, Metin Arik, Ricardo Gobato, Tolga Yarman, Clarification of “Overall Relativistic Energy” According to Yarman's Approach”, Parana Journal of Science and Education, v. 4, n. 8, 2018, pp. 1-10.

[87] Sufia Zaman, Utpal Pal, Ricardo Gobato, Alekssander Gobato, Abhijit Mitra, “The Changing Trends of Climate in Context to

Indian Sundarbans”, Parana Journal of Science and Education, Vol. 4, No. 7, 2018, pp. 24-28.

[88] Suresh Kumar Agarwal, Sitangshu Roy, Prosenjit Pramanick, Prosenjit Mitra, Ricardo Gobato and Abhijit Mitra. Parana Journal of Science and Education. Vol. 4, No. 5, 2018, pp. 15-20.

[89] Ricardo Gobato and Marcia Regina Risso Gobato, “Evidence of Tornadoes Reaching the Countries of Rio Branco do Ivaí and Rosario de Ivaí, Southern Brazil on June 6, 2017”, Climatol Weather Forecasting 2018, 6: 4. DOI: 10.4172/2332-2594.1000242.

[90] Ricardo Gobato. “New Nano-Molecule Kurumi and Raman Spectroscopy using ab initio, Hartree-Fock Method” Am J Biomed Sci & Res. 2019-2 (4). AJBSR. MS. ID. 000594. DOI: 10.34297/AJBSR.2019.02.000594.

[91] D. L. Graf, Rhodochrosite, Crystallographic tables for the rhombohedral carbonates, American Mineralogist 46 (1961) 1283-1316.

[92] E. N. Maslen, V. A. Streltsov, N. R. Streltsova, N. Ishizawa, Electron density and optical anisotropy in rhombohedral carbonates. III. Synchrotron X-ray studies of CaCO₃, MgCO₃ and MnCO₃, Acta Crystallographica B51 (1995) 929-939.

[93] R. Wyckoff, The crystal structures of some carbonates of the calcite group, American Journal of Science 50 (1920) 317-360.

[94] D. Marcus, D. E. Hanwell, D. C. Curtis, T. V. Lonie, E. Zurek, G. R. Hutchison, “Avogadro: An advanced semantic chemical editor, visualization, and analysis platform” Journal of Cheminformatics 2012, 4: 17.

[95] J. Cioslowski, Phys. Rev. Lett., 1989, 62, 1469.

[96] Paul von Ragu Schleyer, Encyclopedia of computational chemistry, New York, J. Wiley, 1998.

[97] Mulliken, R. S. “Electronic Population Analysis on LCAO-MO Molecular Wave Functions. I”. The Journal of Chemical Physics. (1955). 23 (10): 1833-1840. Bibcode: 1955JChPh. 23.1833M. doi: 10.1063/1.1740588.

[98] W. J. Stevens, H. Basch, and M. Krauss, “Compact effective potentials and efficient shared-exponent basis-sets for the 1st-row and 2nd-row atoms,” J. Chem. Phys., 81 (1984) 6026-33. DOI: 10.1063/1.447604.

[99] W. J. Stevens, M. Krauss, H. Basch, and P. G. Jasien, “Relativistic compact effective potentials and efficient, shared-exponent basis-sets for the 3rd-row, 4th-row, and 5th-row atoms,” Can. J. Chem., 70 (1992) 612-30. DOI: 10.1139/v92-085.

[100] T. R. Cundari and W. J. Stevens, “Effective core potential methods for the lanthanides,” J. Chem. Phys., 98 (1993) 5555-65. DOI: 10.1063/1.464902.

[101] Amir Shahram Yousefi Kashi, Samira Khaledi, Mohammad Houshyari, “CT Simulation to Evaluate of Pelvic Lymph Node Coverage in Conventional Radiotherapy Fields Based on Bone and Vessels Landmarks in Prostate Cancer Patients”, Iran J Cancer Prev. 2016; 9 (3): e6233.

[102] Amir Shahram Yousefi Kashi, Abolfazl Razzaghdoust, Afshin Rakhsha, “A Comparative Study of Treatment Toxicities Between FOLFOX 4 and Modified FOLFOX 6 in Iranian Colorectal Cancer Patients”, Iran J Cancer Prev. 2017; 10 (1): e9429.

[103] Amir Shahram Yousefi Kashi, Sharareh Yazdanfar, Mohammad-Esmaeil Akbari, Afshin Rakhsha, "Triple Negative Breast Cancer in Iranian Women: Clinical Profile and Survival Study", *Int J Cancer Manag.* 2017; 10 (8): e10471.

[104] Amir Shahram Y. Kashi, Rezvan Montazeri, Afshin Rakhsha, "Clinical Outcome and Prognostic Factors in Iranian Breast Cancer Patients After Neoadjuvant Chemotherapy: A Comparative Matched Study", *Int J Cancer Manag.* 2018; 11 (5): e67739.

[105] Afshin Rakhsha, Amir Anvari, Abolfazl Razzaghdoust, Amir Shahram Yousefi Kashi, "Clinical Outcome and Prognostic Factors for Very Young Patients with Breast Cancer: A Comparative Matched Single Institution Study in Iran", *Int J Cancer Manag.* 2017; 10 (9): e11772.

[106] Afshin Rakhsha, Amir Shahram Yousefi Kashi, Seied Mohsen Hoseini, "Evaluation of Survival and Treatment Toxicity with High-Dose-Rate Brachytherapy with Cobalt 60 In Carcinoma of Cervix", *Iran J Cancer Preven.* 2015; 8 (4): e3573.

[107] A. Sh. Yousefi Kashi, B. Mofid, H. R. Mirzaei, P. Azadeh, 2010. "Overall Survival and Related Prognostic Factors in Metastatic Brain Tumors Treated with Whole Brain Radiation Therapy", *Research Journal of Medical Sciences*, Volume: 4, Issue: 3, Page No.: 213–216.

How to cite this article:

Authors Name. Alireza Heidari. Hartree-Fock methods analysis protonated rhodochrosite crystal and potential in the elimination of cancer cells through synchrotron radiation using Small-Angle X-Ray Scattering (SAXS), Ultra-Small Angle X-Ray Scattering (USAXS), Fluctuation X-Ray Scattering (FXS), Wide-Angle X-Ray Scattering (WAXS), Grazing-Incidence Small-Angle X-Ray Scattering (GISAXS), Grazing-Incidence Wide-Angle X-Ray Scattering (GIWAXS) and Small-Angle Neutron Scattering (SANS). AJAN 2020;1(1): 1-8
DOI: <https://doi.org/10.5281/zenodo.3757944>